ORCIDs:
Emily R. Featherston: 0000-0003-1338-6611
Hannah R. Rose: 0000-0002-7982-2001
Molly J. McBride: 0000-0003-3832-1355
Amie K. Boal: 0000-0002-1234-8472
Joseph A. Cotruvo, Jr.: 0000-0003-4243-8257

This file contains the Supplementary Experimental Section, Supplementary Tables S1-S6, Supplementary Figures S1-S14, and Supplementary References.

SUPPLEMENTARY EXPERIMENTAL SECTION

SUPPLEMENTARY TABLES

SUPPLEMENTARY FIGURES

SUPPLEMENTARY REFERENCES

SUPPLEMENTARY EXPERIMENTAL SECTION

Cloning of XoxG. *M. extorquens* AM1 *xoxG* was obtained from IDT as a 608-bp gBlock gene fragment, codon optimized for expression in *E. coli* using IDT's online codon optimization tool. The gBlock (**Table S4**) contained a 5' NdeI restriction site (5'-AATACATATG…-3', where ATG is the *xoxG* start codon) and a 3' EcoRI restriction site (5'-…TAAGAATTCAATA-3', where TAA is the *xoxG* stop codon). The gBlock (250 ng) was digested with NdeI and EcoRI (20 U each) for 1 h, and the enzymes were inactivated by incubation at 65 °C for 20 min. pET-24a (2 μg) was digested with NdeI and EcoRI (20 U each) and, following gel electrophoresis (1% agarose), the vector fragment was excised and purified using the Zymoclean Gel DNA Recovery Kit (Genesee Scientific). The *xoxG* insert was ligated into the digested vector (3:1 insert:vector) using T4 DNA ligase according to the manufacturer's protocol. Transformants were screened for insert by colony PCR (GoTaq Green, Promega, or OneTaq Quick-Load, NEB) and the correct insert confirmed by DNA sequencing at the Penn State Genomics Core Facility.

Determination of extinction coefficients of XoxG. The absorption spectra and extinction coefficients of the oxidized and reduced forms of XoxG were determined as described by Barr and Guo.[1] Briefly, a spectrum of the oxidized protein was acquired (240-800 nm) in 30 mM MOPS, pH 7.2 (Buffer F). Using a pipettor, a few grains of sodium dithionite were added to fully reduce the protein. Dithionite does not contribute to the spectrum at >390 nm. The spectrophotometer was blanked on a 1:1 mixture of Buffer F and Solution A (0.2 M NaOH, 40% (v/v) pyridine, 500 μM potassium ferricyanide), and a spectrum was acquired for a 1:1 mixture of Solution A and ~20 μM XoxG in Buffer F. To this solution, 5 μL Solution B (0.5 M sodium dithionite, 0.5 M NaOH) was added and mixed, and a spectrum was acquired immediately and every minute until stable. The heme concentration was determined using ε_{550nm} = 30.27 mM^{-1} cm^{-1} for $(pyridine)_2$-heme *c*. After accounting for dilutions, the extinction coefficients of XoxG in the oxidized and reduced states were calculated from this value. At the isosbestic point (413 nm), ε = 128 $mM^{-1}cm^{-1}$. Maximum absorptions for the reduced form were at 418 nm (ε_{418nm} = 157 $mM^{-1}cm^{-1}$) and 553 nm (ε_{553nm} = 25.8 $mM^{-1}cm^{-1}$).

XoxG crystallography. A solution of XoxG was exchanged into 20 mM MOPS, pH 7, 100 mM KCl, 5 mM acetate and crystallized aerobically. All protein samples were diluted to 5.3 mg/mL (280 μM) prior to crystallization screening. The samples were mixed in a 1:1 ratio with a precipitant solution containing 0.2 M sodium acetate, 0.1 M phosphate-citrate, pH 4.2, and 20% (w/v) PEG 8000. Large, red, rod-shaped crystals were obtained using the hanging drop vapor diffusion method after one week of incubation at room temperature. Crystals were mounted in rayon loops and flash-frozen in liquid nitrogen without additional cryoprotectant.

The crystallographic dataset used for structure determination was collected at the Berkeley Center for Structural Biology at the Advanced Light Source (Lawrence Berkeley National Laboratory), and processed with the HKL2000 package.[2] Phase information was obtained by single-wavelength (1.6984 Å) anomalous diffraction methods. A diffraction dataset collected at 1.698 Å (Fe *K*-edge peak) was analyzed with the program autoSHARP[3] to locate a single heavy atom site (FOM = 0.398, phasing power = 1.0) corresponding to the native iron cofactor of XoxG. Interpretable electron density maps were obtained after solvent flattening and density modification. An initial auto-built model generated with ARP/wARP[4] was further modified and refined using Coot[5] and Refmac5,[6] respectively. Final refinements were carried out in Phenix.[7]

Structures were validated and analyzed for Ramachandran outliers with the Molprobity server.[8] Figures were prepared with the PyMOL molecular graphics software package (Schrödinger, LLC). XoxG crystallizes in the $P6_222$ space group and contains one monomer in the asymmetric unit. The final model consists of residues 31-134, 140-194, and a single heme cofactor (including one Fe ion).

Cloning of XoxJ. *M. extorquens* AM1 *xoxJ* was obtained as a 872-bp gBlock gene fragment, codon optimized for expression in *E. coli* using IDT's online codon optimization tool (**Table S4**). The gBlock contained a 5' NdeI restriction site (5'-AATACATATG…-3', where ATG is the *xoxJ* start codon) and a 3' XhoI restriction site (5'-…TAACTCGAGAATA-3', where TAA is the *xoxJ* stop codon). The gBlock (400 ng) digested with NdeI and XhoI (20 U each) for 1 h, and the enzymes were inactivated by incubation at 65 °C for 20 min. pET-24a (2 μg) was digested with NdeI and XhoI (20 U each) and, following gel electrophoresis (1% agarose), the vector fragment was excised and purified using the Zymoclean Gel DNA Recovery Kit (Genesee Scientific). The *xoxJ* insert was ligated into the digested vector (3:1 insert:vector) using T4 DNA ligase according to the manufacturer's protocol. Transformants were screened for insert by colony PCR (GoTaq Green, Promega) and the correct insert confirmed by DNA sequencing at the Penn State Genomics Core Facility.

Expression and purification of SeMet-labeled XoxJ. A single colony of *E. coli* BL21(DE3) transformed with pET24a-XoxJ was used to inoculate 100 mL of LB-Km, which was grown for ~16 h at 37 °C with shaking at 220 rpm. From this culture, 20 mL were centrifuged at 7000 × *g* for 7 min at 4 °C and resuspended in an equal volume of 1× M9 salts, supplemented with 1 mM $MgSO_4$, 0.1 mM $CaCl_2$, and 0.4% glucose, containing 50 μg/mL Km. This suspension was used to inoculate a 2 L culture in the same medium (in a 6 L flask). The culture was grown at 37 °C with shaking at 200 rpm. At OD_{600nm} ~ 0.55 (~7.5 h), a pre-mixed solution of amino acids (200 mg each L-phenylalanine, L-lysine, and L-threonine; 100 mg each L-valine, L-leucine, L-isoleucine, and seleno-L-methionine, dissolved in 1×M9 salts) was added to the culture. After 15 min, IPTG was added to a final concentration of 0.2 mM and the shaker temperature was lowered to 18 °C. After 16 h, the cells were pelleted by centrifugation for 7 min at 7000 × *g*, 4 °C, yielding ~3.5 g cell paste per L culture. The cell pellets were used immediately to harvest the periplasmic fraction. Purification was identical to XoxJ except for the inclusion of 1 mM DTT in all buffers beginning from the extraction step (incubation with 5 mM $MgSO_4$, 1 mM DTT), and 5 CV was sufficient to elute the SeMet-XoxJ from the gravity-flow phenyl sepharose column. SeMet-labeled XoxJ eluted from the HiPrep Phenyl FF column at 16-9% sat. $(NH_4)_2SO_4$. The protocol yielded ~1 mg SeMet-XoxJ per L culture.

XoxJ crystallography. SeMet-XoxJ was further purified for crystallography by size exclusion chromatography on a HiLoad 16/600 Superdex 200 size exclusion column equilibrated in 50 mM Tris, 150 mM NaCl, pH 7.2, with 1 mM DTT. Crystals of XoxJ were grown from ~25 mg/mL solution in 20 mM MOPS pH 7.3. XoxJ crystallized in two conditions: 1) 0.1 M Tris pH 8.5 and 18-20% PEG 8000; and 2) 0.1 M Tris pH 9.0 and 18-20% (*v/v*) PEG 6000. Crystals were generated via the hanging drop vapor diffusion method at room temperature by mixing together 1 μL of the well solution in a 1:1 μL ratio with the protein solution. Small, flat, rectangular-shaped crystals appeared within 1-2 weeks of incubation at room temperature.

SeMet XoxJ crystals from condition **1** selected for x-ray diffraction analysis were soaked in a cryoprotectant solution consisting of freshly prepared well solution supplemented with 30% (v/v) ethylene glycol for 1-2 min prior to harvesting in rayon loops and flash-freezing in liquid N_2. Native XoxJ crystals from condition **2** were generated via co-crystallization with 1 molar equiv. $LaCl_3$. Flat, rectangular crystals were soaked for 1 h in a solution containing 1.25 mM PQQ, 50 mM HEPES pH 7.6, 20% PEG 6000, and 20 % ethylene glycol. Samples were mounted in rayon loops and flash frozen in liquid N_2.

Initial phase information was obtained from a SeMet-XoxJ crystal by single-wavelength anomalous diffraction methods using diffraction datasets collected at the Se absorption peak (0.9791 Å). After initial processing in HKL2000,[2] the program Crank2[9] (within CCP4) was used to locate the positions of three Se sites (out of three predicted) per XoxJ protomer (FOM = 0.2394). Interpretable electron density maps were obtained after solvent flattening and density modification. An initial auto-built model was generated with Buccaneer[10] and was further modified and refined using Coot[5] and Refmac5[6] respectively. This initial model was used to phase native datasets via molecular replacement in Phaser MR.[11]

XoxJ crystallized in the $P12_11$ space group with one molecule in the asymmetric unit. The final model, which was solved at 2.27 Å resolution, consists of residues 37-80, 83-88, 94-100, 108-169, 177-224, 227-237, 241-273, 48 water molecules, and 2 molecules of ethylene glycol. We note that while XoxJ was crystallized in the presence of 1 molar equiv. $LaCl_3$ and soaked with 1.25 mM PQQ, we did not observe electron density in the final structure for either of these components. Regions of the protein with missing electron density correspond to disordered loops.

Mass spectrometry. XoxG and XoxJ (~10 μM, 100 μL) was exchanged into water using a 0.5 mL Zeba spin column (Thermo Fisher), according to the manufacturer's protocol. The intact protein was analyzed by MALDI-TOF MS in linear positive-ion mode on an Ultraflextreme mass spectrometer (Bruker Daltonics) at the Penn State Proteomics and Mass Spectrometry Facility.

Generation, expression, and purification of XoxJ-W200F. The W200F variant of XoxJ was constructed from pET24a-XoxJ using primers W200F-KLD-for and W200F-KLD-rev (**Table S6**), using the KLD Enzyme Mix, according to the manufacturer's protocol. The sequence was confirmed by DNA sequencing at the Penn State Genomics Core Facility. Expression and purification of XoxJ-W200F was performed identically to that for the wt protein, yielding 1 mg per L culture. Protein concentration was determined using $\varepsilon_{280nm} = 28.5\ mM^{-1}\ cm^{-1}$.[12]

Spectrofluorometric PQQ binding assays with XoxJ. Fluorescence titrations were performed with an excitation wavelength of 290 nm and emission data were acquired at 320-350 nm, with 0.5 nm steps, 0.4 s averaging time, 2.5 nm excitation and 5 nm emission slits, and high PMT setting. In a typical experiment, the cuvette contained ~1 μM XoxJ (wildtype or W200F) in 600 μL Buffer E. The absorbance at 280 nm of the sample was acquired using a UV-visible spectrophotometer in order to determine the protein concentration. After acquisition of 2-3 fluorescence spectra in order to obtain an accurate baseline, PQQ was added in 0.5 or 1 μL aliquots (up to 25 μL total) from a solution of ~200 μM PQQ (determined spectrophotometrically using $\varepsilon_{322nm} = 8963\ M^{-1}\ cm^{-1}$)[13], the sample was mixed by inversion and equilibrated for 30 s and the spectrum was recorded. Longer incubation times did not yield significantly different results. The final concentration of PQQ was ~8 μM. The cuvette was washed with 6 M HCl, water, and acetone after each use. The significant absorption of PQQ in the range of the measurements necessitated

correction for the inner filter effect prior to further analysis. After correction of the emission at 335 nm at each titration point for volume change, the data were analyzed as described by Mertens and Kägi.[14] Briefly, the natural log of each fluorescence intensity value (F) was plotted against PQQ concentration, resulting in a plot that approached a constant decreasing slope at higher PQQ concentrations. At these later points, the slope of the line was determined and this line was subtracted from the overall plot, yielding a plot of ln F_{corr}, F corrected for the inner filter effect (absorption of the excitation beam by PQQ), versus PQQ concentration. From ln F_{corr}, F_{corr} was determined for each titration point.

SUPPLEMENTARY TABLES

Table S1. Protein yields, metal contents, and A_{280nm}/A_{359nm} ratios for La-, Ce-, and Nd-XoxFs

	La-XoxF	Ce-XoxF	Nd-XoxF
Yield (mg/L culture)	0.23	0.26	0.33
A_{280nm}/A_{359nm}	11.8	13.8	10.8
Metal content (equiv. per monomer) [a]	0.94	0.81	1.55

[a] determined by ICP-MS. **Figure S1** supports the interpretation that the super-stoichiometric levels of Nd in the Nd-XoxF sample are in part due to co-purification of Nd-LanM with Nd-XoxF.

Table S2. Data collection and refinement statistics for the x-ray structure of XoxG

	Fe anomalous XoxG
Data collection	
Space group	$P6_222$
Wavelength (Å)	1.6984
Cell dimensions	
a, *b*, *c* (Å)	95.84, 95.84, 80.41
α, β, γ (°)	90.0, 90.0, 120.0
Resolution (Å)	50-2.71 (2.76-2.71)
R_{merge}	0.124 (1.242)
R_{pim}	0.020 (0.256)
$I / \sigma I$	39.2 (3.5)
$CC_{1/2}$	0.999 (0.898)
Completeness (%)	98.6 (97.4)
Redundancy	37.7 (22.4)
Refinement	
Resolution (Å)	50-2.71 (2.76-2.71)
No. reflections	6236
R_{work} / R_{free}	0.1937/0.2484
No. atoms	
Protein	1252
Ligand/ion	43
Water	0
B-factors	
Protein	40.467
Ligand/ion	19.996
Water	-
R.m.s. deviations	
Bond lengths (Å)	0.007
Bond angles (°)	0.969
Molprobity clashscore	4.38 (100^{th} percentile)
Rotamer outliers (%)	0
Ramachandran favored (%)	94.2

*Values in parentheses are for highest-resolution shell.

Table S3. Data collection and refinement statistics for x-ray structures of XoxJ

	SeMet XoxJ	XoxJ
Data collection		
Space group	$P2_12_12_1$	$P12_11$
Wavelength (Å)	0.9791	1.0332
Cell dimensions		
a, *b*, *c* (Å)	49.4070, 67.2030, 76.1730	49.900, 51.7590, 51.2410
α, β, γ (°)	90.0, 90.0 90.0	90.0, 98.23, 90.0
Resolution (Å)	50.0-2.25 (2.31-2.25)	50.00-2.27 (2.30-2.27)
R_{merge}	0.183 (0.783)	0.088 (0.674)
R_{pim}	0.038 (0.295)	0.037 (0.304)
$I / \sigma I$	23 (2.0)	19.6 (2.3)
$CC_{1/2}$	0.343	0.955
Completeness (%)	83.07 (32.18)	93.69 (56.10)
Redundancy	20.3 (6.1)	5.4 (4.8)
Refinement		
Resolution (Å)		50.71-2.27
No. reflections		11410
R_{work} / R_{free}		0.2393/0.27490
No. atoms		
Protein		1663
Ligand/ion		42
Water		8
B-factors		
Protein		38.607
Ligand/ion		33.260
Water		41.985
R.m.s. deviations		
Bond lengths (Å)		0.002
Bond angles (°)		0.532
Molprobity clashscore		2.06 (100^{th} percentile)
Rotamer outliers (%)		0.00
Ramachandran favored (%)		96.45

*Values in parentheses are for highest-resolution shell.

Table S4. Amino acid sequences of *M. extorquens* AM1 XoxG and XoxJ, and gBlocks for their expression in *E. coli*. The regions encoding the signal peptides are shown in red, and the restriction sites are underlined in the gBlocks. In the *M. extorquens* AM1 genome, the underlined Leu (TTG) is annotated as the start codon, but we used the in-frame ATG codon 39 nucleotides prior as the start codon for heterologous expression. XoxJ has a secondary signal peptide cleavage site after D31 (**Figure S10**). The first and last residues visible in the x-ray crystal structures are P31 and L195 (XoxG) and V37 and E273 (XoxJ).

>*M. extorquens* XoxG
MKRTALLGLV GAALLGAVPA ATVAFAQDAK PELANKLDPN AKEIDEPVLK AATAAKEEDG
KYFDKDGHPT FHITNDGKKV DWFTYSGYRR YHAECHVCHG PDGMGSTYAP ALKDSLKRLS
YEEFYGILAG GKQEISNTAN QVMPAFGDNK NVMCYANDLY VYLRARAAGA WGRARPGEKE
DKPESAKTVE KECLGG

>XoxG gBlock
aataCATATGAAACGCACCGCCCTTTTAGGGTTAGTGGGCGCGGCATTGTTAGGTGCGGTACCGGCGGCTACGGTTG
CTTTTGCTCAAGACGCCAAGCCAGAACTGGCTAATAAGTTGGACCCTAACGCGAAAGAGATTGACGAACCTGTTCTT
AAGGCCGCCACAGCGGCTAAGGAGGAAGACGGAAAATATTTTGACAAAGATGGGCACCCAACTTTCCATATTACAAA
TGATGGGAAAAAGGTAGATTGGTTTACGTATTCGGGCTATCGCCGCTACCATGCGGAGTGTCACGTGTGCCACGGGC
CAGACGGGATGGGCTCGACATACGCGCCAGCTTTGAAAGACTCGCTGAAACGCCTGTCGTACGAGGAGTTTTACGGT
ATCCTTGCGGGTGGCAAGCAAGAAATTTCTAACACCGCGAACCAGGTGATGCCAGCCTTTGGCGATAACAAGAACGT
GATGTGCTACGCAAACGACCTGTACGTTTATCTTCGTGCCCGCGCTGCGGGTGCCTGGGGTCGTGCGCGTCCCGGCG
AAAAGGAGGATAAGCCTGAATCCGCGAAGACGGTTGAGAAGGAGTGTTTAGGGGGCTAAgaattcatta

>*M.extorquens* XoxJ
MTRSSAPVSV AVAALLLSAG ARPAHAQHLP DLVTQDVLRV CSDPGNMPFS ERKGGGFENK
IAQIVADELK VKLRYYWLTQ GPGFVRNTLG TGLCDLIIGT SGGDIVQATN PYYRSAYVLV
ARKGELADLK RLDDPRLKDR QIGIIAGTPP SNRLSELKLV GERIHAYAPY AFGAERKHQT
VAAEVIADLA EKKIDVAILW GPAAGWLAKQ SGVPMDVVPL LHEPGRPPLT FRVSMGVRHN
ENDWKRSLNT VLRKRKADIE AVLREYEVPL LAEEDTKPLD AADE

>XoxJ gBlock
aataCATATGACGCGCTCTTCGGCGCCTGTGAGCGTCGCGGTAGCAGCCCTGCTGTTGAGTGCAGGTGCGCGTCCTG
CTCATGCTCAGCACCTGCCGGACCTTGTAACTCAGGACGTGCTCCGTGTGTGCTCCGACCCGGGCAATATGCCGTTT
AGCGAACGCAAAGGCGGCGGTTTTGAAAACAAAATTGCGCAAATCGTTGCGGACGAATTGAAAGTCAAATTGCGCTA
TTATTGGCTGACCCAGGGCCCAGGTTTTGTCCGCAATACCCTGGGGACGGGTCTGTGCGATCTGATCATTGGTACTT
CTGGTGGCGACATTGTTCAGGCAACAAACCCGTATTATCGTTCTGCTTACGTGCTGGTGGCGCGTAAAGGCGAACTC
GCTGATCTGAAACGCCTGGATGATCCTCGCCTCAAGGATCGTCAGATTGGAATTATCGCAGGTACGCCCCCGTCCAA
CCGTCTGTCAGAACTCAAGCTTGTGGGCGAGCGCATTCATGCCTATGCACCGTATGCTTTTGGTGCGGAACGTAAAC
ACCAAACCGTGGCGGCGGAAGTGATCGCTGATTTAGCGGAGAAAAAGATCGACGTTGCAATCTTGTGGGGTCCTGCG
GCTGGTTGGCTGGCGAAACAGTCGGGCGTGCCAATGGACGTCGTACCGCTGCTGCACGAACCAGGCCGTCCGCCTTT
AACGTTCCGCGTTAGTATGGGCGTTCGTCACAACGAAAACGACTGGAAACGCTCGCTCAACACCGTTCTGCGCAAAC
GCAAAGCAGATATCGAAGCAGTGCTTCGCGAATACGAGGTCCCACTGTTAGCAGAAGAAGATACTAAACCGTTGGAT
GCCGCAGATGAATAACTCGAGaata

Table S5. Plasmids used in this study

Name	Notes	Source
pEC86	Cm^R	Ref. [15]
pET24a	Km^R	Novagen
pET24a-XoxG	XoxG inserted into NdeI/EcoRI-digested pET24a	This work
pET24a-XoxJ	XoxJ inserted into NdeI/XhoI-digested pET24a	This work
pET24a-XoxJ-W200F	W200F variant of XoxJ	This work

Table S6. Primers used for cloning and sequencing

Name	Sequence[a]
W200F-KLD-for	5'-TGCAATCTTGTTTGGTCCTGCGG-3'
W200F-KLD-rev	5'-ACGTCGATCTTTTTCTCCG-3'
Sequencing primers	
T7P	5'-TAATACGACTCACTATAGGG-3'
T7T	5'-GCTAGTTATTGCTCAGCGG-3'

[a] Mutated nucleotides underlined

SUPPLEMENTARY FIGURES

Figure S1. SDS-PAGE analysis of Ln-XoxFs purified from *M. extorquens* AM1, following size exclusion chromatography. Lane 1: Molecular weight marker. Lane 2: La-XoxF. Lane 3: Ce-XoxF. Lane 4: Nd-XoxF. The most prominent co-purifying bands at 13 kDa and 16 kDa were identified by mass spectrometry analysis of the excised gel bands. The 13 kDa band was identified as a 10 kDa chaperonin (GroS), perhaps suggesting a role of this ATP-driven folding chaperone in folding and activation of XoxF. The 16 kDa band was identified as the formaldehyde-oxidizing enzyme, 5,6,7,8-tetrahydromethanopterin hydrolyase (Fae), a cytosolic enzyme and therefore possibly an artifact. Based on our previous studies,[16] the band at just above the 10 kDa marker is assigned as the Ln-binding protein lanmodulin (LanM), which we have observed co-purifying in a Ln-bound form with XoxF. This band is more intense in the Nd-XoxF sample, which may account, at least in part, for the observed >1 equiv. Nd in the Nd-XoxF sample.

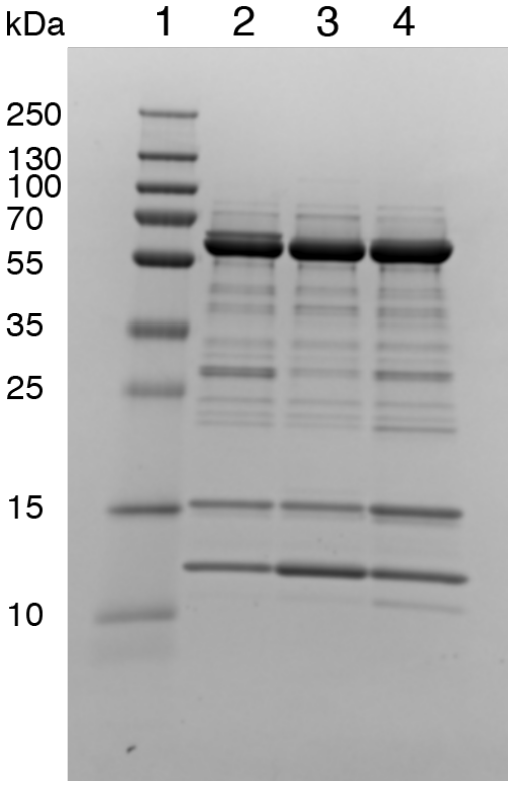

Figure S2. UV-visible absorption spectra of La-, Ce-, and Nd-XoxFs (~0.8 µM dimer), purified from native levels in *M. extorquens*. The absorption feature at 350-360 nm and shoulder at ~410 nm are indicative of PQQ-containing MDHs.

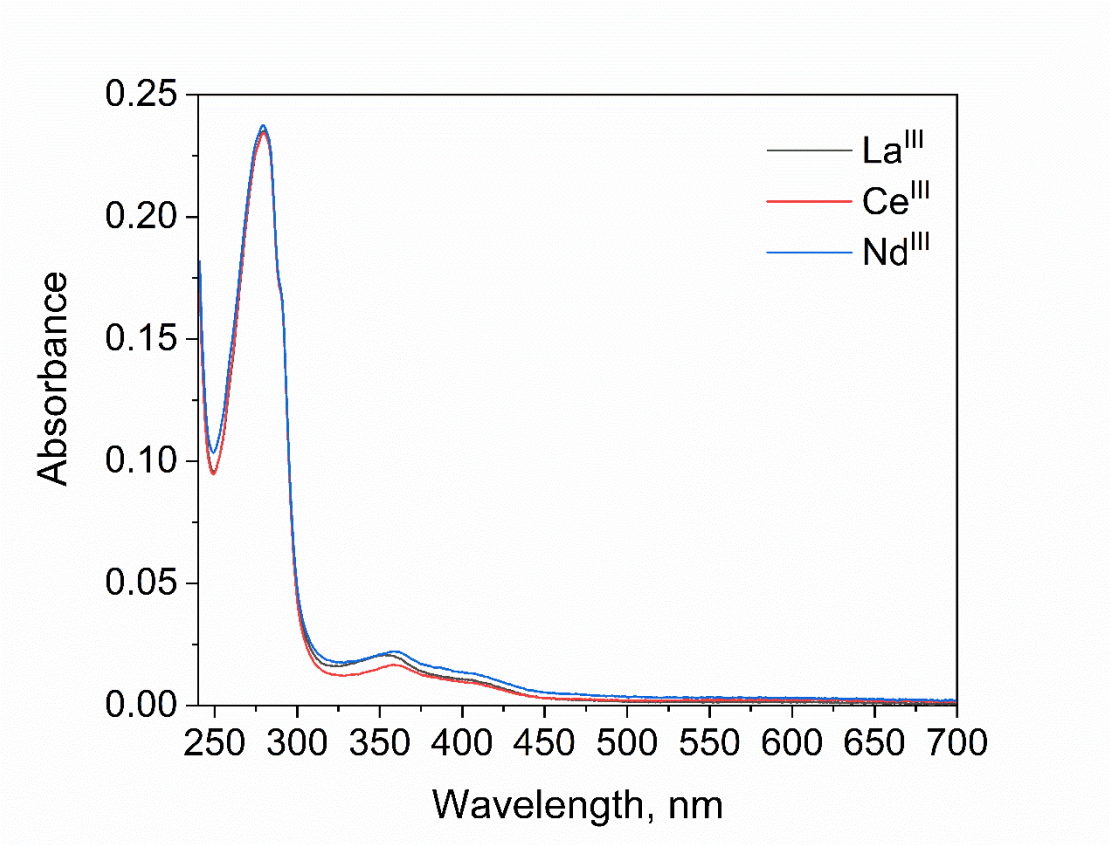

Figure S3. SDS-PAGE analysis of purification of XoxG heterologously expressed in *E. coli*. Lane 1: molecular weight marker; lanes 2 and 3: samples pre- and post-induction with 1 μM IPTG; lane 4: periplasmic extract; lane 5: phenyl sepharose elution; lanes 6 and 7: DEAE flowthrough (first and second CV); lane 8: Q sepharose flowthrough (20 mM MOPS, 1 mM EDTA, pH 8.2); lanes 9 and 10: Q sepharose elution. This gel used samples from a slightly different purification protocol from that described in the Experimental Procedures section, in which the DEAE column was run first and the Q sepharose step was judged to not to be necessary. Comparable purity was achieved by the stated, optimized protocol.

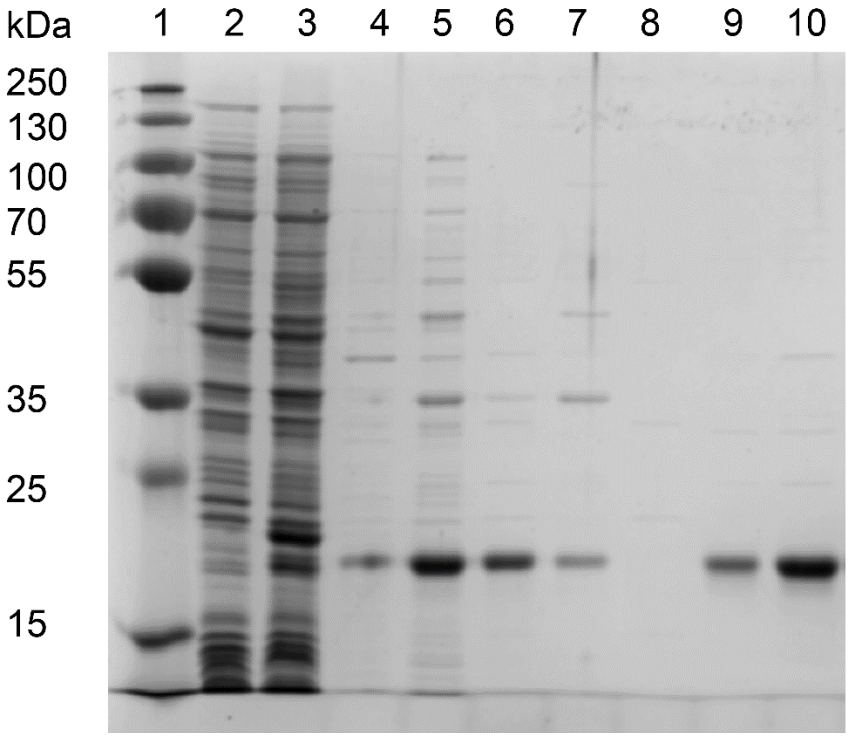

Figure S4. Linear MALDI-TOF mass spectrum of XoxG. The *m/z* = +1 peak at 19456.145 Da corresponds to cleavage before Gln27 and a covalently bound heme *c* (expected mass: 18840.01 + 618.50 = 19458.51 Da). See **Table S4** for XoxG sequence.

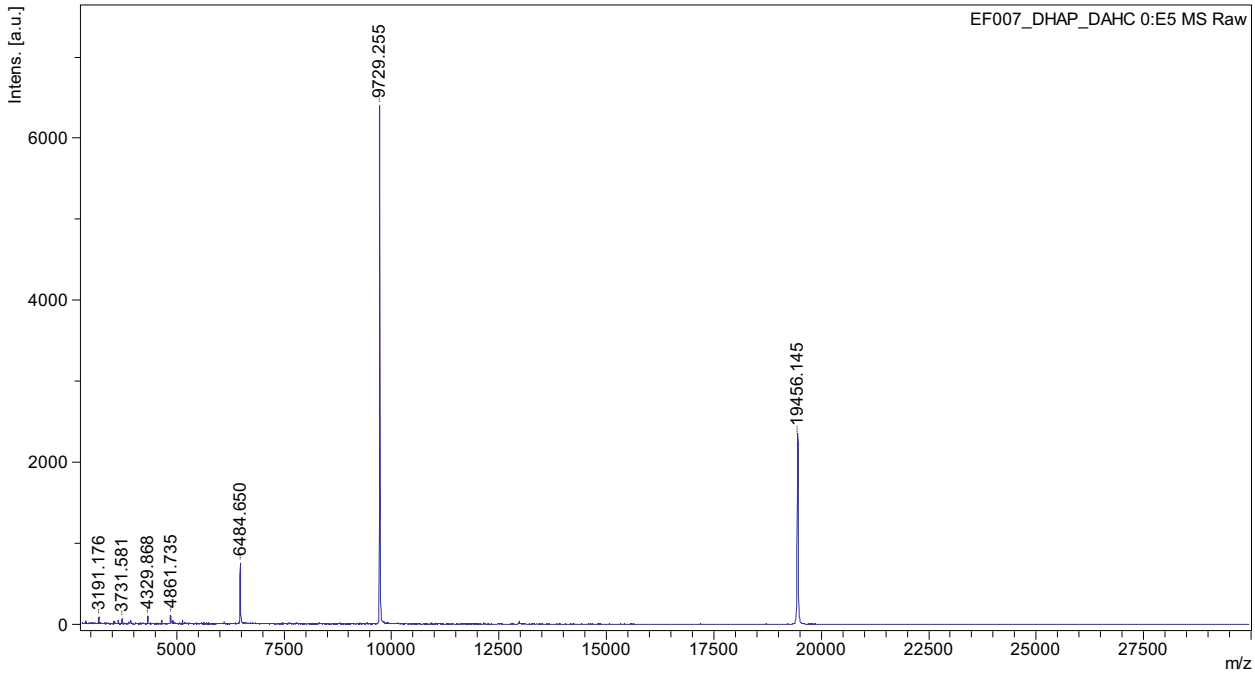

Figure S5. UV-visible absorbance spectrum of oxidized XoxG from 600-800 nm. The feature at 695 nm is indicative of Met ligation of the heme Fe^{III}.

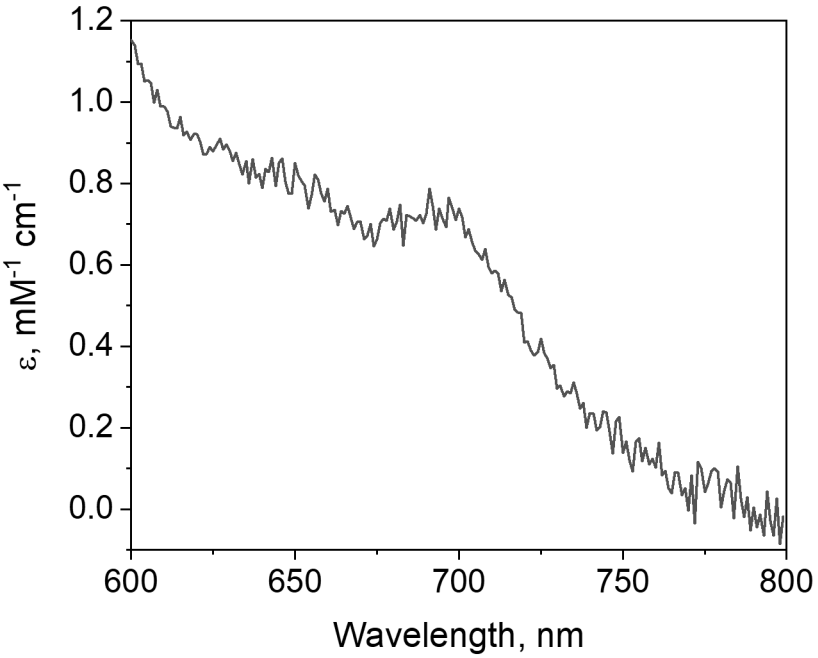

Figure S6. Determination of the XoxG reduction potential from the results in **Figure 2B**. Using the concentrations of oxidized and reduced DCPIP and XoxG determined at each titration timepoint as described in the main text, the Nernst plot (see Efimov et al.[17]) was generated, noting that reduction of DCPIP is a two-electron process and reduction of XoxG is a one-electron process. The E_m of XoxG was determined by the sum of the E_m of DCPIP (+217 mV) and the y-intercept of the regression line. The equation of the line for the data shown is: $y = 0.86x - 46$.

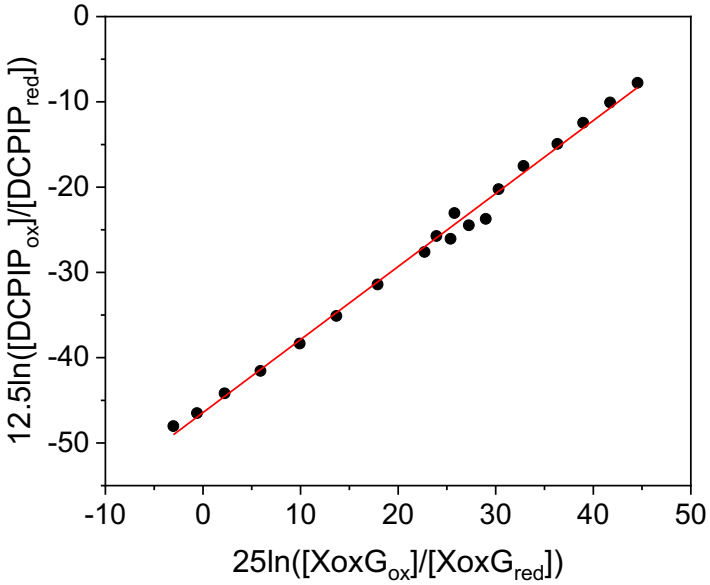

Figure S7. Comparison of XoxG with other *c*-type cytochromes. (A) *M. extorquens* XoxG (this work), (B) *M. extorquens* MxaG (PDB ID: 2C8S), (C) *R. marinus* cytochrome *c* (PDB ID: 3CP5), and (D) *S. cerevisiae* cytochrome *c* (PDB ID: 1YCC). All proteins contain a His-/Met-ligated ferric heme in solution. The MxaG cofactor is coordinated by a second His side chain in the x-ray structure. XoxG contains the three conserved core helices (I, III, V) in the immediate vicinity of the heme cofactor.

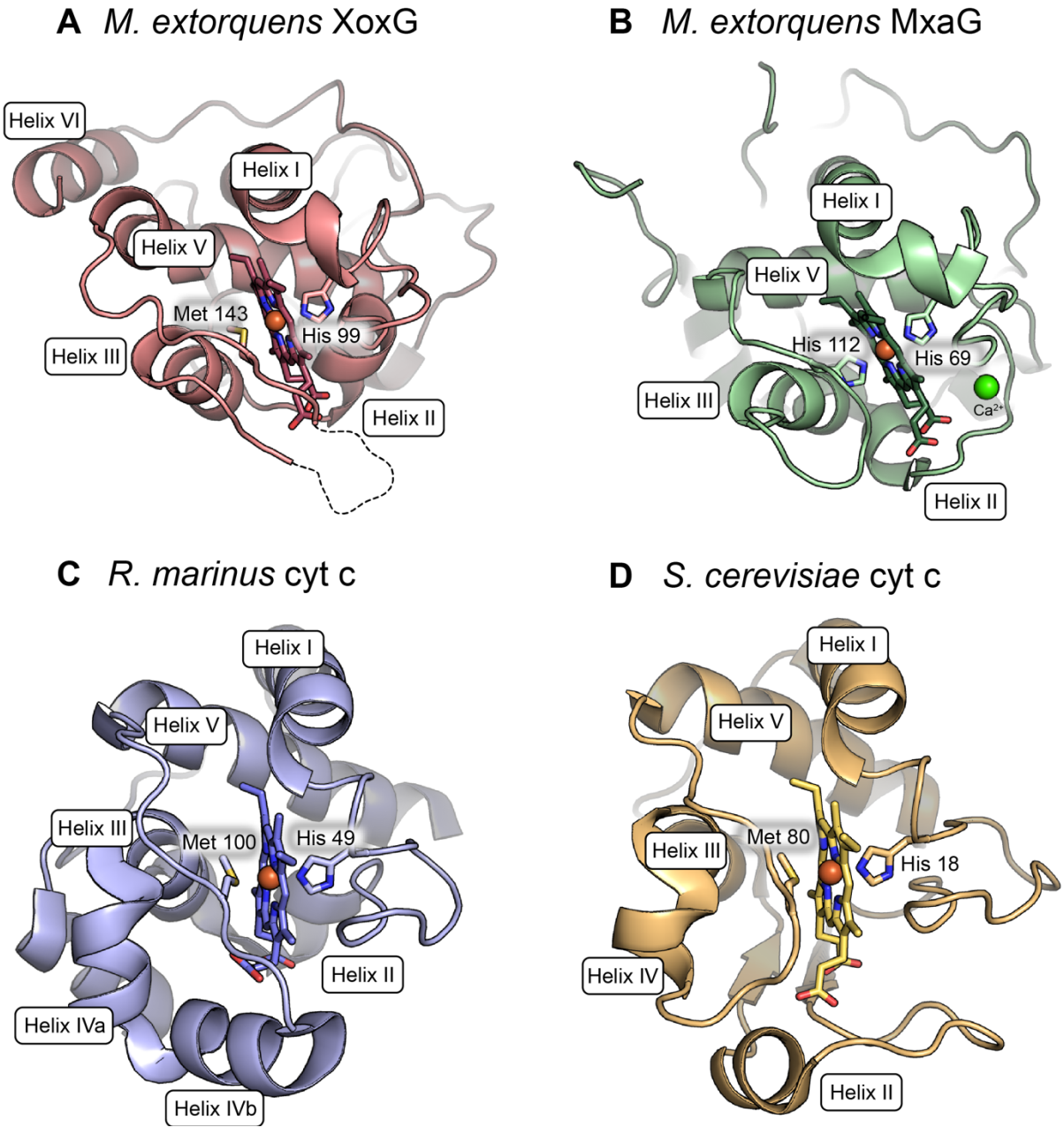

Figure S8. Cartoon representation colored by *B*-factor of (A) XoxG (this work), and (B) MxaG (PDB ID: 2C8S). High *B*-factors usually represent flexible regions of the protein. MxaG has high *B*-factors at the N-terminus and the Met(His) ligand loop, which contributes a His ligand to the heme in this structure rather than the Met ligand observed in solution. There is little or no density for residues 105-108, immediately following the unbound Met ligand. The combination of the His ligand artifact in MxaG and disorder in the corresponding loop region in XoxG presents challenges in comparing the heme environment for the two proteins.

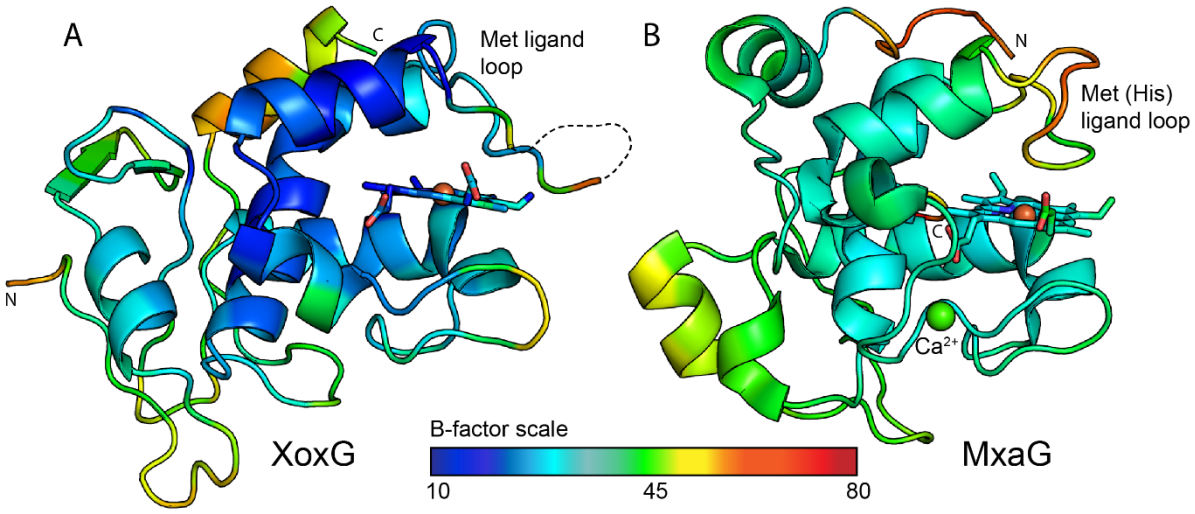

Figure S9. Docking model of XoxG with homology model of its redox partner, XoxF. The docking model was generated using the crystal structure of a PQQ-dependent alcohol dehydrogenase natively fused to its *c*-type cytochrome (PDB code: 1YIQ)[18] as template (A), by alignment of XoxG with the cytochrome *c* domain and a homology model of *M. extorquens* XoxF generated from the crystal structure of *M. fumariolicum* XoxF (4MAE,[19] **Figure S13**) with the alcohol dehydrogenase domain. PQQ was modeled in the XoxF homology model based on its placement within the 1YIQ structure. Selected amino acid residues and the heme/PQQ cofactors are shown in stick format. Cerium, calcium, and iron ions are shown as spheres. Insets show a cutaway view of the interface between the cytochrome and PQQ domains. (B) The docking model suggests that the interaction between XoxG and XoxF could be mediated through flexible loops located at the surfaces of both proteins, including the partially disordered extended loop near Met 130. In this model, the closest distance between the reactive C5 position of PQQ and the heme edge is ~16 Å. Two cysteine residues (Cys 103 and Cys 104) in the XoxF homology model form a disulfide bridge near the PQQ moiety and Ce^{III} ion, and at the interface with XoxG (11 Å from the heme edge). The docking model for XoxF-XoxG includes a clash involving the XoxG loop near His 99 and the C-terminal domain of XoxF (inset, bottom center).

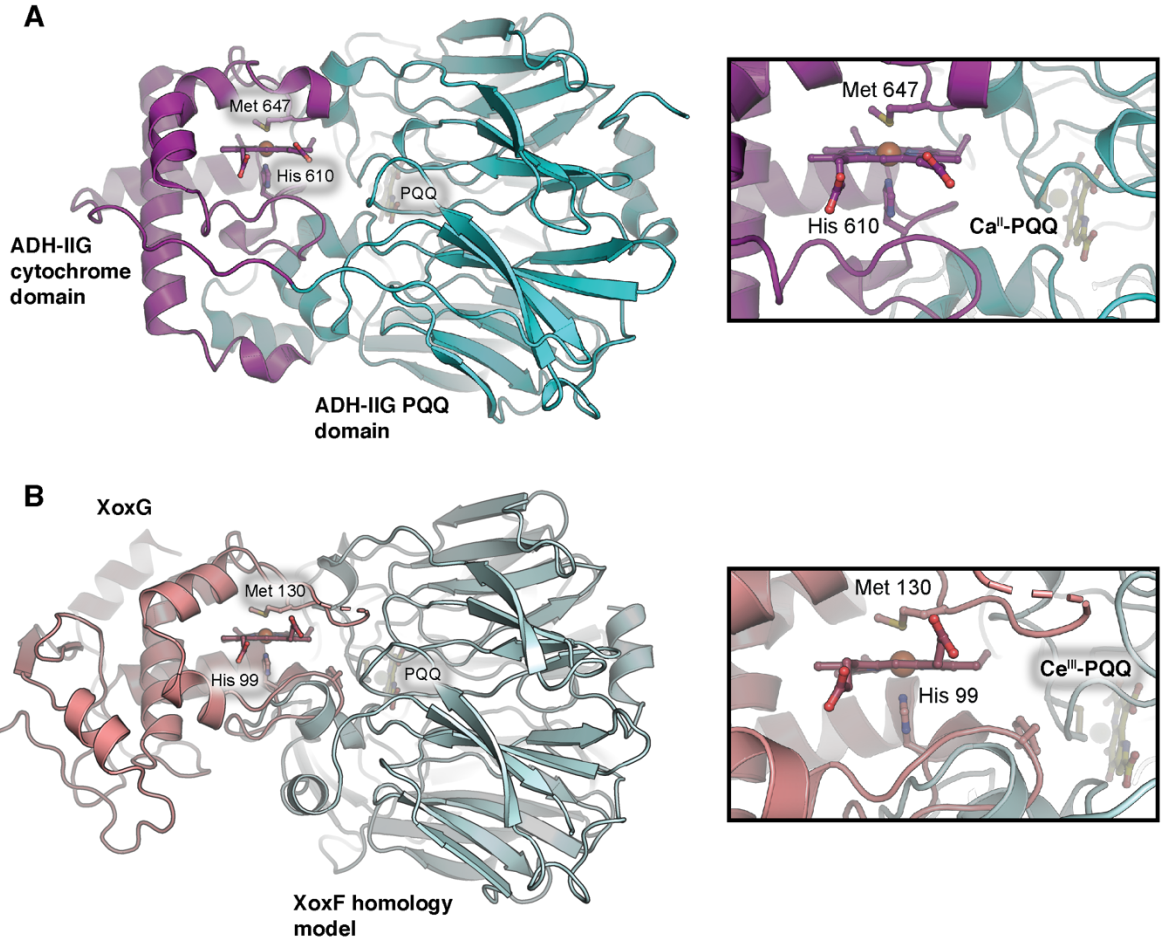

Figure S10. Linear MALDI-TOF mass spectrum of XoxJ. The *m/z* = +1 peaks at 28601.592 and 28012.805 Da correspond to cleavage before Gln27, the site predicted by SignalP 4.0,[20] and before Leu32 (expected masses: 28597.81 and 28007.17, respectively). These two cleavage products were consistently observed in XoxJ preparations. On an SDS-PAGE gel, the corresponding bands were both present in the whole-cell post-induction sample, indicating that the lower, major band was not a result of proteolysis during purification but rather an alternative cleavage site in *E. coli*. See **Table S4** for the XoxJ sequence.

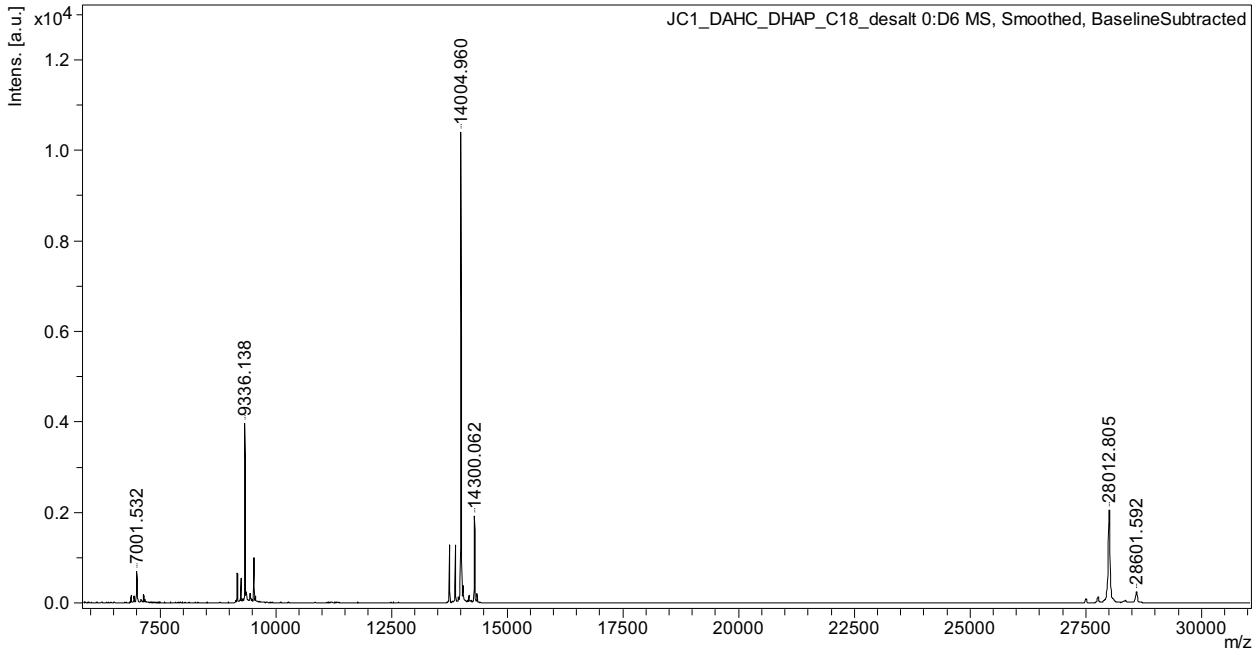

Figure S11. Fluorometric titrations of XoxJ (wildtype and W200F) with PQQ. (A) Raw fluorescence (average of emission at 332-336 nm) of 1 μM XoxJ titrated with 0-8 μM PQQ (λ_{ex} = 290 nm). The data are not corrected for the inner filter effect due to absorption of PQQ at the excitation wavelength. (B) The same data as in (A), but after correction for the inner filter effect as described in the Supplementary Experimental Section. The data indicate that quenching of W200 fluorescence is primarily responsible for the effect of added PQQ on wt XoxJ fluorescence.

A

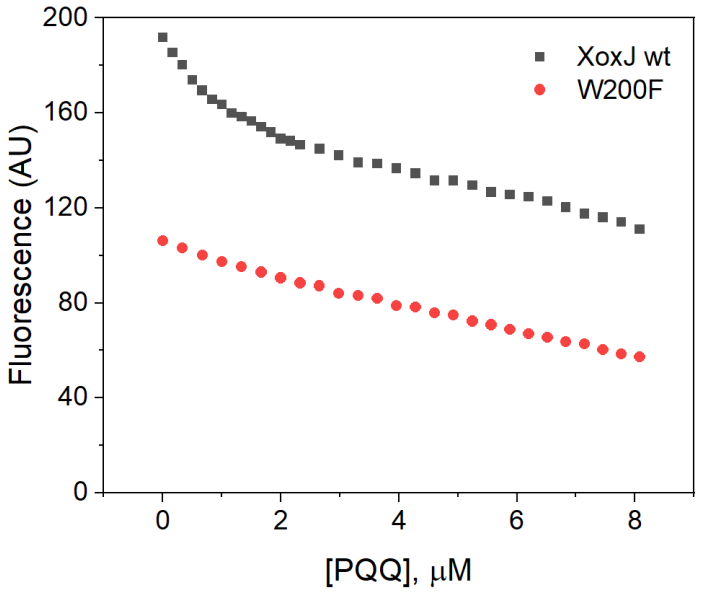

B

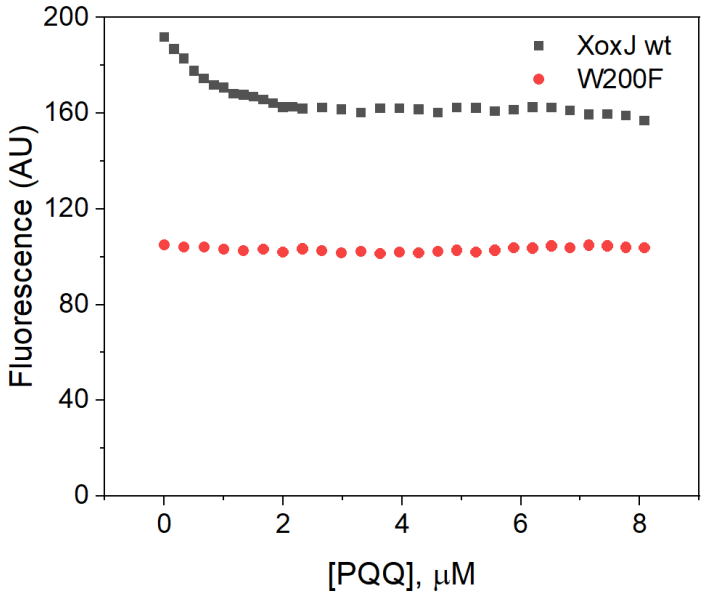

Figure S12. Elution of holo- and apo-XoxF from a size exclusion column, demonstrating monomerization of XoxF upon cofactor removal. La-XoxF (200 µL, 19 µM) was incubated overnight with 10 mM EGTA and loaded to a Superdex 200 10/300 GL column (23.6 mL volume) using a 500 µL loop. The column was pre-equilibrated and run in 20 mM MOPS, 100 mM KCl, 1 mM EGTA, pH 7.0, at a flow rate of 0.5 mL/min. Protein was detected by A_{280nm} and PQQ by A_{346nm}. The elution times for the two XoxF peaks are 13.74 and 15.16 min, corresponding to apparent molecular weights of 107 and 51 kDa, respectively, calibrated using the GE Gel Filtration Calibration Kit LMW. Expected molecular weights of XoxF dimer and monomer are 126 and 63 kDa, respectively.

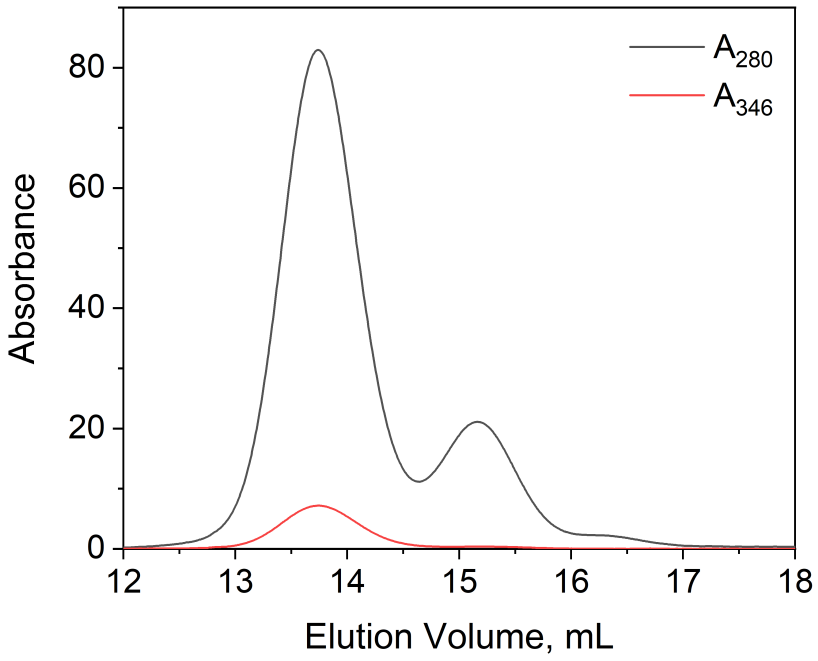

Figure S13. Organization of the final β sheet in XoxF suggests a putative route for PQQ and Ln cofactor insertion. (A) Homology model of *M. extorquens* XoxF, generated from the crystal structure of *M. fumariolicum* XoxF (4MAE[19]). The Ce^{III} ions are shown in tan spheres and the PQQ cofactor in yellow sticks. The N-terminal region of the protein, through the first β strand (N21-S68) is shown in purple. The final three β strands and the helical domain (M539-P599) are in cyan. Together, these β strands form the final β sheet in the protein, and they are positioned at the dimer interface. (B) Enlarged view of one subunit of the dimer, showing that the helical domain is positioned directly over the active site. (C) Amino acid sequence of XoxF. The signal peptide is underlined (cleavage site verified by Nakagawa et al.[21]) and the segments discussed above are colored in purple and cyan, respectively.

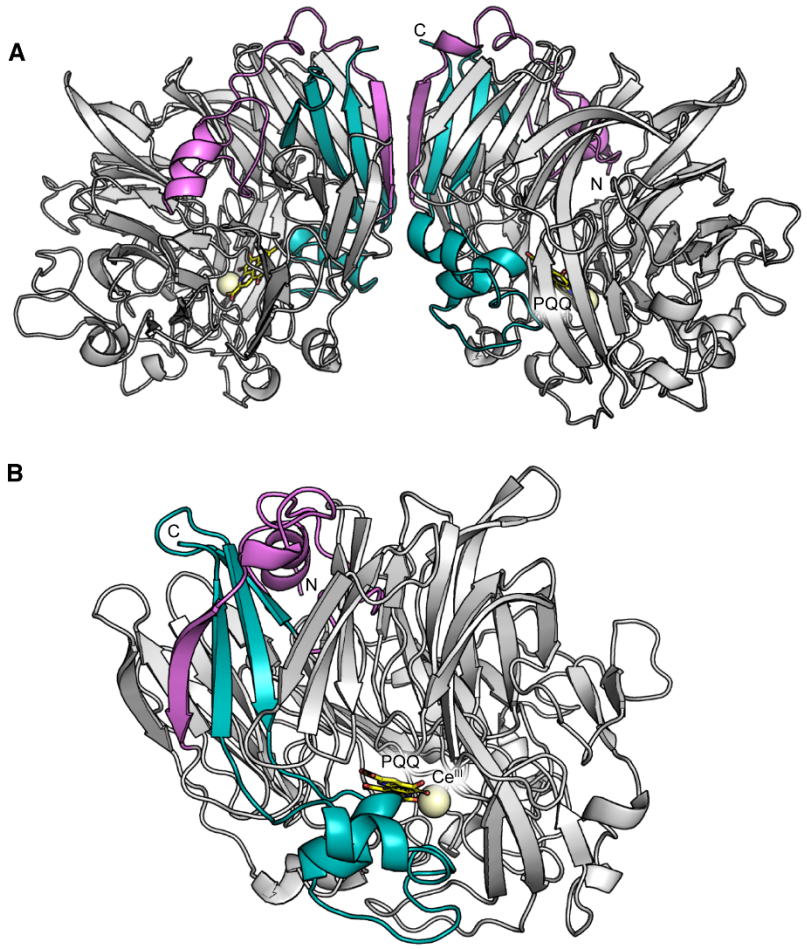

C

>*M. extorquens* XoxF

MRAVHLLALG AGLAAASPAL ANESVLKGVA NPAEQVLQTV DYANTRYSKL DQINASNVKN
LQVAWTFSTG VLRGHEGSPL VVGNIMYVHT PFPNIVYALD LDQGAKIVWK YEPKQDPSVI
PVMCCDTVNR GLAYADGAIL LHQADTTLVS LDAKSGKVNW SVKNGDPSKG ETNTATVLPV
KDKVIVGISG GEFGVQCHVT AYDLKSGKKV WRGYSIGPDD QLIVDPEKTT SLGKPIGKDS
SLKTWEGDQW KTGGGCTWGW FSYDPKLDLM YYGSGNPSTW NPKQRPGDNK WSMTIWARNP
DTGMAKWVYQ MTPHDEWDFD GINEMILTDQ KFDGKDRPLL THFDRNGFGY TLDRATGEVL
VAEKFDPVVN WATKVDLDKG SKTYGRPLVV SKYSTEQNGE DVNSKGICPA ALGTKDQQPA
AFSPKTGLFY VPTNHVCMDY EPFRVTYTPG QPYVGATLSM YPAPGSHGGM GNFIAWDNLQ
GKIKWSNPEQ FSAWGGALAT AGDVVFYGTL EGFLKAVDSK TGKELYKFKT PSGIIGNVMT
YEHKGKQHVA VLSGVGGWAG IGLAAGLTDP NAGLGAVGGY AALSSYTNLG GQLTVFSLPN
N

Figure S14. Potential complementarity of the C-terminal region of XoxF with XoxJ. (A) *Top,* C-terminal peptide from XoxF (residues G554-P599, see **Figure S13**). *Bottom,* cavity from XoxJ. The dimensions of both XoxF and the cavity were estimated in PyMOL and do not include the side chains from XoxF. (B) Two views of the C-terminal part of XoxF docked in the central cavity of XoxJ (domain 1 at top). The XoxF domain was manually rotated and translated in PyMOL. Although some side chain clashes exist, this model simply emphasizes that with minor backbone arrangement the helical domain of XoxF fits into the ligand-binding cavity of XoxJ. Similarly, rearrangement of the loop between the last helix and strand (T587-G591) would reasonably position the strand to intercalate into the disordered portion of domain 1 of XoxJ. Furthermore, domain 1 of XoxJ lacks 3 strands of the five-strand β sheet normally present in PBPs. We speculate that this structural difference could provide a location for the C-terminal β strands of XoxF to interact with XoxJ.

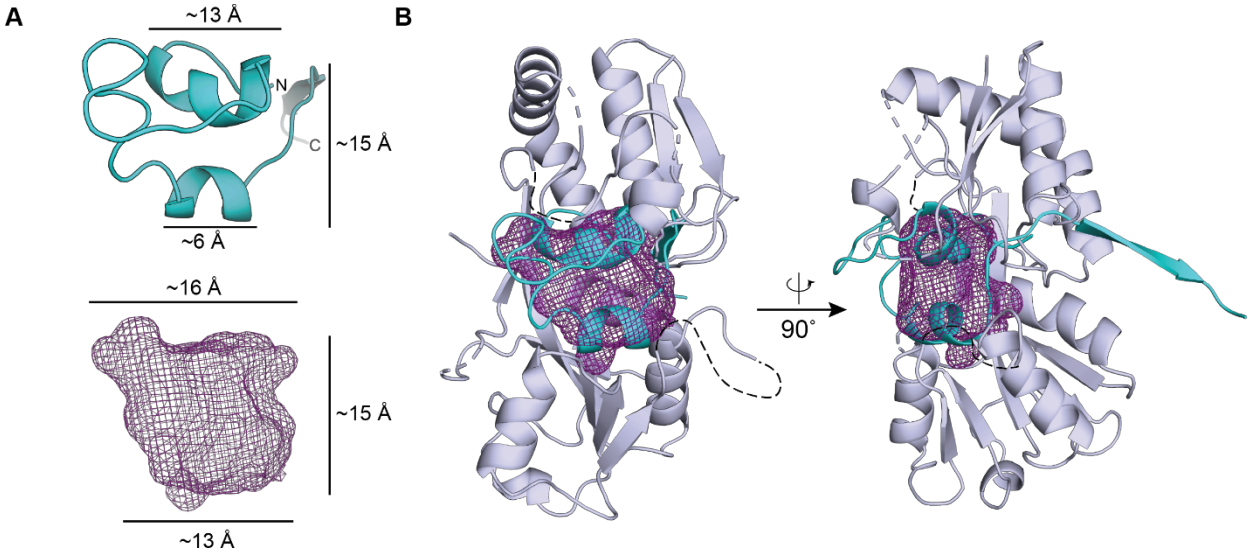

SUPPLEMENTARY REFERENCES

[1] I. Barr, F. Guo, *Bio-Protocol* **2015**, *5*, http://www.bio-protocol.org/e1594.
[2] Z. Otwinowski, W. Minor, *Methods Enzymol.* **1997**, *276*, 307-326.
[3] C. Vonrhein, E. Blanc, P. Roversi, G. Bricogne, *Methods Mol. Biol.* **2007**, *364*, 215-230.
[4] G. Langer, S. X. Cohen, V. S. Lamzin, A. Perrakis, *Nat. Protoc.* **2008**, *3*, 1171-1179.
[5] P. Emsley, K. Cowtan, *Acta Crystallogr., Sect. D: Biol. Crystallogr.* **2004**, *60*, 2126-2132.
[6] G. N. Murshudov, A. A. Vagin, E. J. Dodson, *Acta Crystallogr., Sect. D: Biol. Crystallogr.* **1997**, *53*, 240-255.
[7] P. D. Adams, P. V. Afonine, G. Bunkóczi, V. B. Chen, I. W. Davis, N. Echoo ls, J. J. Headd, L.-W. Hung, G. J. Kapral, R. W. Grosse-Kunstleve, A. J. McCoy, N. W. Moriarty, R. Oeffner, R. J. Read, D. C. Richardson, J. S. Richardson, T. C. Terwilliger, P. H. Zwart, *Acta Cryst.* **2010**, *D66*, 213-221.
[8] V. B. Chen, W. B. Arendall, J. J. Headd, D. A. Keedy, R. M. Immormino, G. J. Kapral, L. W. Murray, J. S. Richardson, D. C. Richardson, *Acta Crystallogr., Sect. D: Biol. Crystallogr.* **2010**, *66*, 12-21.
[9] M. D. Winn, C. C. Ballard, K. D. Cowtan, E. J. Dodson, P. Emsley, P. R. Evans, R. M. Keegan, E. B. Krissinel, A. G. Leslie, A. McCoy, S. J. McNicholas, G. N. Murshudov, N. S. Pannu, E. A. Potterton, H. R. Powell, R. J. Read, A. Vagin, K. S. Wilson, *Acta Crystallogr., Sect. D: Biol. Crystallogr.* **2011**, *67*, 235-242.
[10] K. Cowtan, *Acta Crystallogr., Sect. D: Biol. Crystallogr.* **2006**, *62*, 1002-1011.
[11] A. J. McCoy, R. W. Grosse-Kunstleve, L. C. Storoni, R. J. Read, *Acta Crystallogr., Sect. D: Biol. Crystallogr.* **2005**, *61*, 458-464.
[12] E. Gasteiger, C. Hoogland, A. Gattiker, S. Duvaud, M. R. Wilkins, R. D. Appel, A. Bairoch, in *The Proteomics Protocols Handbook* (Ed.: J. M. Walker), Humana Press, Totowa, NJ, **2005**, pp. 571-607.
[13] R. H. Dekker, J. A. Duine, J. Frank, P. E. J. Verweil, J. Westerling, *Eur. J. Biochem.* **1982**, *125*, 69-73.
[14] M. L. Mertens, J. H. R. Kägi, *Anal. Biochem.* **1979**, *96*, 448-455.
[15] E. Arslan, H. Schulz, R. Zufferey, P. Künzler, L. Thöny-Meyer, *Biochem. Biophys. Res. Commun.* **1998**, *251*, 744-747.
[16] J. A. Cotruvo, Jr., E. R. Featherston, J. A. Mattocks, J. V. Ho, T. N. Laremore, *J. Am. Chem. Soc.* **2018**, *140*, 15056-15061.
[17] I. Efimov, G. Parkin, E. S. Millett, J. Glenday, C. K. Chan, H. Weedon, H. Randhawa, J. Basran, E. L. Raven, *FEBS Lett.* **2014**, *588*, 701-704.
[18] H. Toyama, Z. W. Chen, M. Fukumoto, O. Adachi, K. Matsushita, F. S. Mathews, *J. Mol. Biol.* **2005**, *352*, 91-104.
[19] A. Pol, T. R. M. Barends, A. Dietl, A. F. Khadem, J. Eygensteyn, M. S. M. Jetten, H. J. M. Op den Camp, *Environ. Microbiol.* **2014**, *16*, 255-264.
[20] T. N. Petersen, S. Brunak, G. von Heijne, H. Nielsen, *Nat. Methods* **2011**, *8*, 785-786.
[21] T. Nakagawa, R. Mitsui, A. Tani, K. Sasa, S. Tashiro, T. Iwama, T. Hayakawa, K. Kawai, *PLoS ONE* **2012**, *7*, e50480.